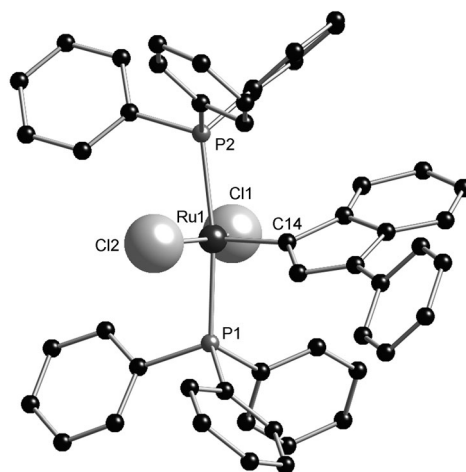


# From Olefin Metathesis Catalyst to Alcohol Racemization Catalyst in One Step\*\*

Simone Manzini, César A. Urbina-Blanco, Albert Poater, Alexandra M. Z. Slawin, Luigi Cavallo, and Steven P. Nolan\*

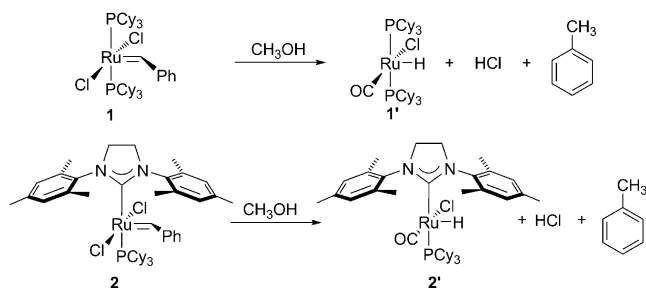
One of the most important challenges in ruthenium-catalyzed olefin metathesis is to increase the stability of the catalysts under the reaction conditions without loss of activity.<sup>[1]</sup> Although most ruthenium-based olefin metathesis catalysts, in the solid state, are stable to oxygen and moisture, they usually readily undergo decomposition in solution.<sup>[2]</sup> Understanding the decomposition routes of catalysts is extremely important as any insight gained in this area can guide catalyst design efforts.

The well-defined and easily accessed  $[\text{RuCl}_2(\text{PPh}_3)_2(3\text{-phenylindenylidene})]$  ( $\mathbf{M}_{10}$ ; Figure 1) complex<sup>[3]</sup> is not efficient in olefin metathesis itself, but is an important synthon used in the preparation of a number of classes of ruthenium-based olefin metathesis catalysts.<sup>[4]</sup> Although slightly stable in solution under anaerobic and anhydrous conditions,  $\mathbf{M}_{10}$  exhibits rapid decomposition in the presence of alcohols. The instability of ruthenium olefin metathesis complexes to alcohols is often encountered. Indeed, in methanol, these complexes are prone to methanolysis and lead to the formation of hydrido carbonyl complexes.<sup>[5]</sup> Examples of such decomposition products ( $\mathbf{1'}$  from  $\mathbf{1}$  and  $\mathbf{2'}$  from  $\mathbf{2}$ ) are



**Figure 1.** X-ray structure of  $\mathbf{M}_{10}$  (H atoms are omitted for clarity). Selected bond lengths [Å] and angles [°]: Ru1–Cl1 1.867(4), Ru1–Cl2 2.3518(12), Ru1–Cl2 2.3741(12), Ru1–P1 2.3851(12), Ru1–P2 2.4021(12); P1–Ru1–P2 170.99(4), Cl1–Ru1–Cl2 156.51(4), Cl1–Ru1–P1 91.15(12), Cl1–Ru1–P2 97.86(12)

presented in Scheme 1. As HCl is generated, these reactions are accelerated by base.<sup>[6]</sup>



**Scheme 1.** Methanolysis decomposition products of the first- and second-generation olefin metathesis precatalysts  $\mathbf{1}$  and  $\mathbf{2}$ , respectively.

As previous reports had examined the benzylidene precursors ( $\mathbf{1}$  and  $\mathbf{2}$ ), we became interested in the influence of an indenylidene moiety, found in  $\mathbf{M}_{10}$ , in such decomposition processes.

As anticipated,  $\mathbf{M}_{10}$  proves unstable in alcohol solution. Analysis of the progress of this decomposition by  $^{31}\text{P}\{^1\text{H}\}$  NMR spectroscopy reveals the appearance of two doublets at  $\delta = 42.3$  and  $48.7$  ppm with a coupling of  $J_{\text{PP}} = 46.1$  Hz, all of which support the formation of a new complex bearing two spectroscopically non-equivalent phosphorus

[\*] S. Manzini, C. A. Urbina-Blanco, Prof. A. M. Z. Slawin, Prof. Dr. S. P. Nolan  
EaStCHEM School of Chemistry, University of St Andrews  
St Andrews, KY16 9ST (UK)  
E-mail: snolan@st-andrews.ac.uk  
Homepage: <http://chemistry.st-andrews.ac.uk/staff/spn/group>

Dr. A. Poater  
Catalan Institute for Water Research (ICRA), H2O Building  
Scientific and Technological Park of the University of Girona  
Girona (Spain)  
and  
Institut de Química Computacional, Departament de Química  
University of Girona, Girona (Spain)

Prof. L. Cavallo  
Department of Chemistry and Biology, University of Salerno  
Fisciano (Italy)

[\*\*] The research leading to these results has received funding from the European Community's Seventh Framework Programme (FP7/2007-2013) under grant agreement no. CP-FP 211468-2 EUMET. S.P.N. is a Royal Society Wolfson Research Merit Award holder. L.C. thanks BSC (QCM-2010-2-0020), and the HPC team of Enea for the use of the ENEA-GRID and the HPC facilities, and CRESCO, in Portici (Italy) for access to remarkable computational resources. A.P. thanks the Spanish MICINN for a Ramón y Cajal contract (RYC-2009-04170) and the European Commission for a Career Integration Grant (CIG09-GA-2011-293900).

Supporting information for this article is available on the WWW under <http://dx.doi.org/10.1002/anie.201106915>.

centers. The  $^1\text{H}$  NMR spectrum does not, however, indicate the formation of a hydride species.

To completely exclude the possible formation of a hydridocarbonyl complex, a series of tests were conducted to confirm that **M**<sub>10</sub> does promote alcohol oxidation. A reaction of **M**<sub>10</sub> in isopropyl alcohol with a stoichiometric amount of triethylamine (to sequester any possible HCl formed) reveals an improved decomposition process. The formation of triethylammonium chloride and acetone were confirmed by spectroscopy, thus supporting the effective alcohol oxidation.

The novel microcrystalline ruthenium complex was characterized by NMR spectroscopy, and surprisingly the data suggest that the indenyl moiety is still coordinated to the ruthenium center, but in a different coordination mode. Indeed, in the  $^{13}\text{C}$  NMR spectrum, there was no resonance between  $\delta = 240$  and  $330$  ppm,<sup>[7]</sup> a resonance that is characteristic of the alkylidene carbon atom. Therefore to unambiguously confirm the identity of the new ruthenium product formed, single crystals suitable for X-ray diffraction studies were grown by slow diffusion of a  $\text{CH}_2\text{Cl}_2/\text{MeOH}$  (1:10) solution at room temperature (Figure 2).<sup>[3]</sup>

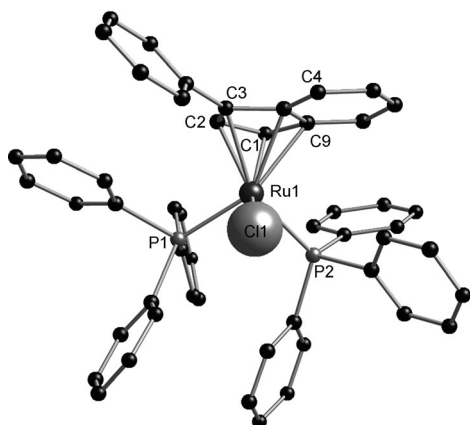
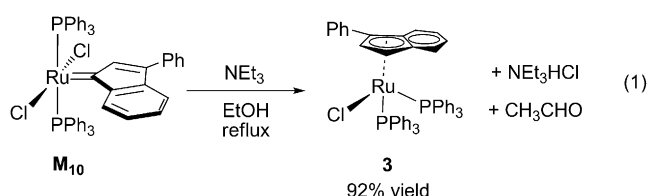


**Figure 2.** X-ray structure of **3** (H atoms are omitted for clarity). Selected bond lengths [Å] and angles [°]: Ru1–Cl1 2.182(5), Ru1–C2 2.194(4), Ru1–C3 2.271(4), Ru1–C4 2.348(4), Ru1–C9 2.345(4), Ru1–P1 2.3430(11), Ru1–P2 2.2960(11), Ru1–Cl1 2.4407(12); P2–Ru1–P1 96.49(4), P1–Ru1–Cl1 92.34(4), P2–Ru1–Cl1 96.82(4).

X-ray analysis of **3** confirms an unusual and unexpected transformation in which **M**<sub>10</sub> is involved in alcohol oxidation and subsequent formation of a new ruthenium complex, wherein the indenylidene moiety rearranges into a  $\eta^5$ -coordinated indenyl in  $[\text{RuCl}(\text{PPh}_3)(\eta^5\text{-3-phenylindenyl})]$  (**3**). Comparing **3** to its ruthenium indenyl congener  $[\text{RuCl}(\text{PPh}_3)_2(\eta^5\text{-C}_9\text{H}_7)]$ ,<sup>[8]</sup> highlights that **3** has a smaller P–Ru–P bond angle ( $96.49(4)^\circ$  for **3** versus  $99.205(18)^\circ$  for indenyl), presumably a result of the steric hindrance of the phenyl substituent on the indenyl.

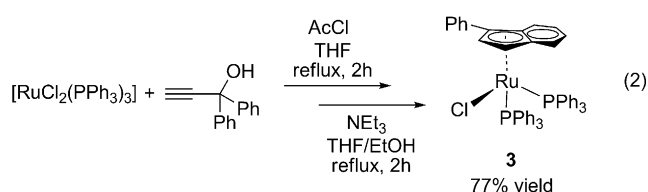
In an optimized protocol, **3** can be obtained quantitatively (92% yield of isolated compound) by refluxing **M**<sub>10</sub> in ethanol for 2 hours in the presence of a stoichiometric amount of triethylamine [Eq. (1)].



Reaction kinetics monitored by  $^{31}\text{P}\{^1\text{H}\}$  NMR spectroscopy permit a determination of the overall rate of the reaction as  $v = k[\text{M}_{10}][\text{EtOH}]$ . Triethylamine is absent from the rate expression. This unusual rearrangement occurs through phosphine dissociation as excess phosphine decreases the rate of the reaction. However the phosphine dissociation does not take place in the rate-determining step as it is zero order in the reaction rate. An Eyring plot permits the determination of following thermodynamic parameters:  $\Delta H^\ddagger = 25.1(2)$  kcal mol<sup>−1</sup>;  $\Delta S^\ddagger = 113(5)$  cal mol<sup>−1</sup> K, and  $E_A = 25.7(2)$  kcal mol<sup>−1</sup>.

To the best of our knowledge, this represents the first example of an indenylidene to indenyl rearrangement. Moreover, this particular rearrangement does not occur for the tricyclohexylphosphine congener,  $[\text{RuCl}_2(\text{PCy}_3)_2(3\text{-phenylindenylidene})]$  (**M**<sub>1</sub>), which decomposes to form the known hydrido carbonyl complex **1'**.

As **M**<sub>10</sub> is easily synthesized from the ruthenium synthon,  $[\text{RuCl}_2(\text{PPh}_3)_3]$ ,<sup>[1c,4b]</sup> and as **3** is easily synthesized from **M**<sub>10</sub>, we reasoned that a one-pot approach leading to **3** from  $[\text{RuCl}_2(\text{PPh}_3)_3]$  might be possible. Gratifyingly, this is the case and **3** can be isolated in 77% yield over two steps [Eq. (2)].

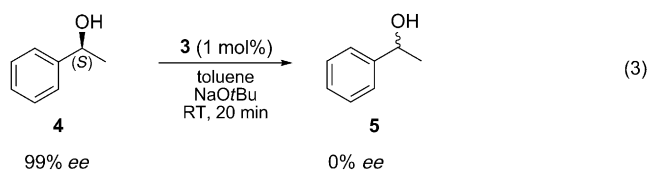


Complex **3**, as expected, is not metathesis active, but the ruthenium complexes are catalytically active in numerous catalytic transformations: alcohol racemization,<sup>[9]</sup> rearrangement of propargylic alcohols,<sup>[10]</sup> cyclization,<sup>[11]</sup> and polymerization, to name a few.<sup>[8,12]</sup> We identified here an opportunity to make use of a decomposition product as an active catalyst in a worthwhile transformation.

Among the transformations mediated by Ru/indenyl complexes, racemization protocols are especially interesting as they are often involved in industrial syntheses to obtain enantiomerically pure compounds.<sup>[13]</sup> This is possible by introducing a racemization catalyst into a kinetic resolution reaction, thus allowing complete conversion of a racemic alcohol into an enantiomerically pure compound [dynamic kinetic resolution process (DKR)].<sup>[14]</sup> As we have recently investigated the racemization of chiral alcohols mediated by related ruthenium complexes,<sup>[15]</sup> **3** was tested in this transformation.

(*S*)-Phenylethanol was selected as a substrate to evaluate the catalytic activity of **3** in the racemization of a chiral

alcohol. The reaction was performed in toluene at room temperature with added sodium *tert*-butoxide to generate the active catalyst [Eq. (3)].



Within 20 minutes, complete racemization was achieved using 1 mol % of the catalyst (10000 ppm). A catalyst loading as low as 10 ppm affords near complete racemization (95 %) in 14 hours at room temperature. Further decrease in the catalyst loading to 1 ppm affords the racemized alcohol in 70 % after 14 hours at room temperature (see the Supporting Information)

DFT calculations permitted assembling all the experimental information into the energy profile shown in Figure 3. To facilitate the computational effort, MeOH was used as the model alcohol.<sup>[16]</sup> The discussed energies have been calculated with the M06 L functional. The same chemical picture, with similar energies, is obtained with the BP86 functional (Figure 3).

The first step corresponds to substitution of one PPh<sub>3</sub> ligand of **M**<sub>10</sub> by a MeOH molecule, a process that is endothermic by 12.2 kcal mol<sup>-1</sup>. The next step corresponds to proton transfer from the coordinated MeOH to a NEt<sub>3</sub> molecule. This transfer requires overcoming the transition-state **A**→**B** at 12.9 kcal mol<sup>-1</sup> above the starting material, and collapsing into intermediate **B**, which is 4.5 kcal mol<sup>-1</sup> above the starting material. The formally anionic intermediate **B** is characterized by a methoxy ligand that is *trans* to the N-heterocyclic carbene (NHC) ligand, with the formally cationic NEt<sub>3</sub>H<sup>+</sup> molecule hydrogen bonded to both the MeO and the

nearby Cl ligand (H...O and H...Cl distances of 2.62 and 2.00 Å, respectively). The Ru–Cl bond involved in the hydrogen bond is 0.1 Å longer than the other Ru–Cl bond. Dissociation of NEt<sub>3</sub>H<sup>+</sup>Cl<sup>-</sup> from the ruthenium center occurs through transition-state **B**→**C**, which sits 24.0 kcal mol<sup>-1</sup> above the starting material. During this step the MeO ligand moves to the coordination position vacated by the leaving Cl ligand, and the ruthenium complex collapses into intermediate **C**, which presents a vacant coordination position *trans* to the NHC ligand. This vacant coordination position can be occupied by the previously dissociated PPh<sub>3</sub> molecule, thus leading to the intermediate **D**, which sits at 1.7 kcal mol<sup>-1</sup> above the starting material. The energy gain associated with PPh<sub>3</sub> coordination is 19.6 kcal mol<sup>-1</sup>. The final steps of the transformation involve first a hydrogen atom transfer from the Me group of the MeO ligand to the ylidene carbon atom of the indenylidene ligand via the transition-state **D**→**E** at 27.6 kcal mol<sup>-1</sup>, thus leading to intermediate **E**, which has an η<sup>1</sup>-coordinated indenyl ligand, and liberates a H<sub>2</sub>CO molecule. The last step of the reaction corresponds to the almost barrierless isomerization of the η<sup>1</sup>-coordinated indenyl ligand of **E** into a η<sup>5</sup>-coordination mode, with formation of the classical piano-stool tetracoordinated ruthenium complex **3**. The overall reaction profile of Figure 3 indicates that the limiting step is transfer of a hydrogen atom of the MeO ligand to the ylidene carbon atom via the transition-state **D**→**E**. This transition state is calculated to lay 27.6 kcal mol<sup>-1</sup> above the starting material, which is in good agreement with the experimental *E*<sub>a</sub> = 25.7 kcal mol<sup>-1</sup>, and is in qualitative agreement with the experimental evidence that NEt<sub>3</sub> does not participate to the rate-determining step. However, the initial proton transfer from MeOH to the Cl ligand, assisted by NEt<sub>3</sub> via transition-state **B**→**C** at 24.0 kcal mol<sup>-1</sup>, is not much lower in energy. The direct transfer from **A** to **C**, in the absence of a nearby NEt<sub>3</sub> molecule, is calculated to cost 39.9 kcal mol<sup>-1</sup>, which clearly indicates the role of NEt<sub>3</sub> in promoting the **M**<sub>10</sub> to **3** transformation.

In conclusion, an unusual indenylidene to indenyl rearrangement has been uncovered, and leads to the rather facile formation of a new ruthenium indenyl complex. This complex, formally a decomposition product from an olefin metathesis catalyst, displays exceptional activity in the racemization of chiral alcohols. The generality of this unusual rearrangement leading to indenyl complexes is presently being investigated in our laboratories.

Received: September 29, 2011  
Published online: December 12, 2011

**Keywords:** alcohols · computational chemistry · rearrangement · ruthenium · structure elucidation

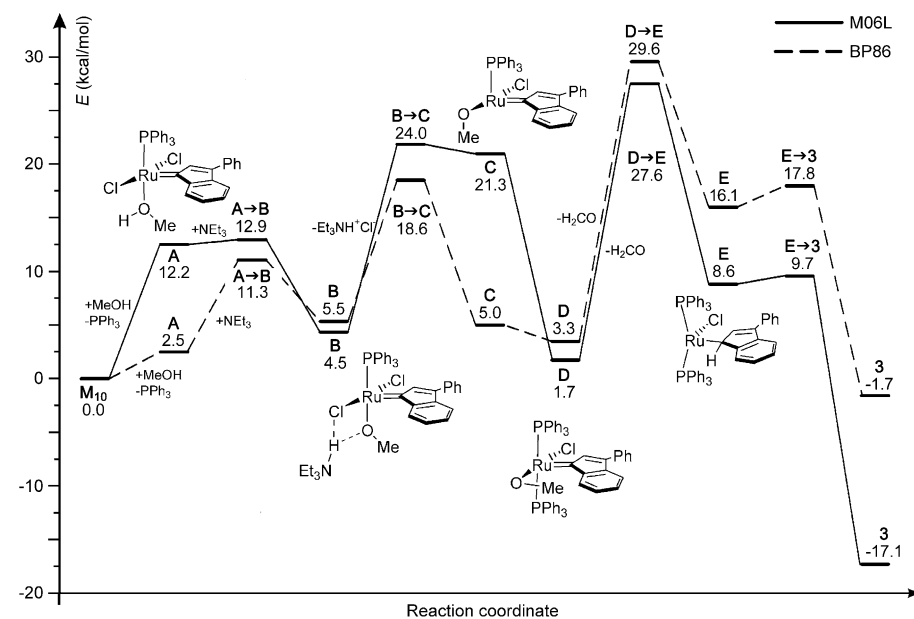


Figure 3. DFT energy profile for the transformation of **M**<sub>10</sub> into **3**.

- [1] a) H. Clavier, F. Caijo, E. Borré, D. Rix, F. Boeda, S. P. Nolan, M. Mauduit, *Eur. J. Org. Chem.* **2009**, 4254–4265; b) F. Boeda, H. Clavier, S. P. Nolan, *Chem. Commun.* **2008**, 2726–2740; c) A. M. Lozano-Vila, S. Monsaert, A. Bajek, F. Verpoort, *Chem. Rev.* **2010**, *110*, 4865–4909; d) C. E. Diesendruck, E. Tzur, N. G. Lemcoff, *Eur. J. Inorg. Chem.* **2009**, 4185–4203.
- [2] a) G. C. Vougioukalakis, R. H. Grubbs, *Chem. Rev.* **2010**, *110*, 1746–1787; b) H. Clavier, K. Grela, A. Kirschning, M. Mauduit, S. P. Nolan, *Angew. Chem.* **2007**, *119*, 6906–6922; *Angew. Chem. Int. Ed.* **2007**, *46*, 6786–6801; c) B. Alcaide, P. Almendros, A. Luna, *Chem. Rev.* **2009**, *109*, 3817–3858.
- [3] CCDC 838203 (**3**) and 838204 (**M<sub>10</sub>**) contain the supplementary crystallographic data for this paper. These data can be obtained free of charge from The Cambridge Crystallographic Data Centre via [www.ccdc.cam.ac.uk/data\\_request/cif](http://www.ccdc.cam.ac.uk/data_request/cif).
- [4] a) C. A. Urbina-Blanco, S. Manzini, J. P. Gomes, A. Doppiu, S. P. Nolan, *Chem. Commun.* **2011**, *47*, 5022–5024; b) E. A. Shaffer, C.-L. Chen, A. M. Beatty, E. J. Valente, H.-J. Schanz, *J. Organomet. Chem.* **2007**, *692*, 5221–5233.
- [5] T. M. Trnka, J. P. Morgan, M. S. Sanford, T. E. Wilhelm, M. Scholl, T.-L. Choi, S. Ding, M. W. Day, R. H. Grubbs, *J. Am. Chem. Soc.* **2003**, *125*, 2546–2558.
- [6] a) M. B. Dinger, J. C. Mol, *Organometallics* **2003**, *22*, 1089–1095; b) N. J. Beach, K. D. Camm, D. E. Fogg, *Organometallics* **2010**, *29*, 5450–5455.
- [7] J. F. Hartwig, *Organotransition Metal Chemistry: from Bonding to Catalysis*, University Science Books, Sausalito, CA, **2010**.
- [8] M. Kamigaito, Y. Watanabe, T. Ando, M. Sawamoto, *J. Am. Chem. Soc.* **2002**, *124*, 9994–9995.
- [9] a) D. Lee, E. A. Huh, M.-J. Kim, H. M. Jung, J. H. Koh, J. Park, *Org. Lett.* **2000**, *2*, 2377–2379; b) J. H. Koh, H. M. Jung, M.-J. Kim, J. Park, *Tetrahedron Lett.* **1999**, *40*, 6281–6284; c) J. H. Koh, H. M. Jeong, J. Park, *Tetrahedron Lett.* **1998**, *39*, 5545–5548; d) F. F. Huerta, Y. R. S. Laxmi, J.-E. Bäckvall, *Org. Lett.* **2000**, *2*, 1037–1040.
- [10] a) B. M. Trost, A. H. Weiss, *Org. Lett.* **2006**, *8*, 4461–4464; b) B. M. Trost, J. Xie, N. Maulide, *J. Am. Chem. Soc.* **2008**, *130*, 17258–17259; c) B. M. Trost, N. Maulide, R. C. Livingston, *J. Am. Chem. Soc.* **2008**, *130*, 16502–16503; d) B. M. Trost, R. C. Livingston, *J. Am. Chem. Soc.* **2008**, *130*, 11970–11978; e) B. M. Trost, R. C. Livingston, *J. Am. Chem. Soc.* **1995**, *117*, 9586–9587; f) B. M. Trost, R. J. Kulawiec, *J. Am. Chem. Soc.* **1993**, *115*, 2027–2036; g) B. M. Trost, A. C. Gutierrez, R. C. Livingston, *Org. Lett.* **2009**, *11*, 2539–2542; h) B. M. Trost, A. Breder, B. M. O’Keefe, M. Rao, A. W. Franz, *J. Am. Chem. Soc.* **2011**, *133*, 4766–4769.
- [11] a) Y. Yamamoto, H. Kitahara, R. Ogawa, H. Kawaguchi, K. Tatsumi, K. Itoh, *J. Am. Chem. Soc.* **2000**, *122*, 4310–4319; b) Y. Yamamoto, H. Kitahara, R. Hattori, K. Itoh, *Organometallics* **1998**, *17*, 1910–1912; c) Y. Yamamoto, T. Arakawa, R. Ogawa, K. Itoh, *J. Am. Chem. Soc.* **2003**, *125*, 12143–12160; d) O. Tutusaus, S. Delfosse, A. Demonceau, A. F. Noels, R. Núñez, C. Viñas, F. Teixidor, *Tetrahedron Lett.* **2002**, *43*, 983–987.
- [12] a) K. Nakatani, T. Terashima, M. Sawamoto, *J. Am. Chem. Soc.* **2009**, *131*, 13600–13601; b) T. K. Goh, J. F. Tan, S. N. Guntari, K. Satoh, A. Blencowe, M. Kamigaito, G. G. Qiao, *Angew. Chem.* **2009**, *121*, 8863–8867; *Angew. Chem. Int. Ed.* **2009**, *48*, 8707–8711; c) S. Ida, T. Terashima, M. Ouchi, M. Sawamoto, *J. Am. Chem. Soc.* **2009**, *131*, 10808–10809.
- [13] E. J. Ebberts, G. J. A. Ariaans, J. P. M. Houbiers, A. Bruggink, B. Zwanenburg, *Tetrahedron* **1997**, *53*, 9417–9476.
- [14] a) F. F. Huerta, A. B. E. Minidis, J.-E. Bäckvall, *Chem. Soc. Rev.* **2001**, *30*, 321–331; b) O. Pàmies, J.-E. Bäckvall, *Chem. Rev.* **2003**, *103*, 3247–3262.
- [15] a) J. Bosson, A. Poater, L. Cavallo, S. P. Nolan, *J. Am. Chem. Soc.* **2010**, *132*, 13146–13149; b) J. Bosson, S. P. Nolan, *J. Org. Chem.* **2010**, *75*, 2039–2043.
- [16] All calculations were performed with the Gaussian09 package at the BP86 GGA level using the SDD ECP on Ru and the SVP basis set on all main group atoms. The reported energies have been obtained via single-point calculations at the M06 L MGGA and BP86 level with the TZVP basis set on main group atoms and an additional diffuse function on Cl and O. Solvent effects, MeOH, were included with the PCM model.